SEISMIC BEHAVIOR OF STEEL FRAMES WITH COMPOSITE GIRDERS

B.Kato (I)
H.Aoki (II)
Y.Tagawa (III)
Presenting Author: Y. Tagawa

SUMMARY

This report presents the seismic behavior of steel frames with composite girders. Nearly full scale moment frame and braced frame are tested under repeated and reversed loading. The experimental results regarding the behaviors of components and frames are described. Hysteresis rules for each component of the frames with composite girders are determined by considering the composite effect of R.C.slab. These individual hysteresis loops are composed to predict hysteresis loops of the test frames. They are compared with the experimental results and discussed.

INTRODUCTION

U.S.-Japan Cooperative Research Program Utilizing Large-Scale Testing Facilities has been recommended for assessing the damage and safety levels of buildings designed using current design practices. Research Program includes full scale tests for a seven-story reinforced concrete building and a six-story steel building. The research program of the steel building has started in 1982 with some support tests for the full scale frame test. This report describes one of them concerning to the seismic behavior of steel frames with composite girders. Nearly full scale moment frame and braced frame picked up from the typical floor level of the six-story steel building are tested under repeated and reversed horizontal loading in order to obtain the restoring-force characteristics which should be used in the pseudo-dynamic loading program in the testing of the six-story full scale steel frame.

TEST SPECIMENS

Fig.-1 illustrates the plan and section of the full scale steel structure, which has 2X2 spans and 6 stories (Ref.1). Two portions, hatched in the section shown in Fig.-1, are taken out from the full scale structure as specimens. The one is an unbraced frame at the third floor, named specimen No.1 in this paper. The other is a braced frame at the sixth floor, named specimen No.2.

The composite slab consists of embossed steel deck 1.6mm thickness, light concrete and 100mm pitch wire mesh of 6mm in diameter, as shown in Fig.-2. Studs are welded on the flange of girders to satisfy the full composite action between R.C.slab and steel girder. The beam-to-column connection in the strong axis direction of the column is the moment connection in which beam flanges are groove welded to column face and beam

(I) Professor of Architecture, University of Tokyo, JAPAN

(II) Professor of Architecture, Yokohama National University, JAPAN

(III) Research Assistant of Architecture, Yokohama National Univ., JAPAN

web is jointed by high-strength bolts, while the shear connection is adopted in the weak axis direction. The end of the diagonal bracing with a square hollow section is welded to beam or column.

The material properties of the concrete and steel are tabulated in Table-1.

TESTING PROCEDURE

The specimen was clumped to the test floor, and the external lateral force was applied by means of two oil jacks with capacity of +50, -100ton load and ±150mm stroke. The setting of the specimen is illustrated in Fig.-3.

As the loading program, displacement amplitudes were decided 1/300, 1/200, 1/120, 1/80, 1/60, 1/40, in terms of relative story displacement angle. The angle of 1/40 is comparable with the maximum deformation predicted by a provisional earthquake response analysis on the full scale structure, assuming the maximum ground acceleration of 350 gal.

TEST RESULTS

Fig.-4 demonstrates the experimental result of the relation between lateral load Q and displacement δ at the upper end of the inner column for the test specimen No.1. At the fourth cycle, local buckling was observed in the flange of the girder near the beam-to-column connection of the outer column. The local distortion grew up with the cyclic loading and the portion finally ruptured. As is observed in this figure, the hysteresis loops are stable.

Fig.-5 shows the Q-δ relation of the test specimen No.2. At the second cycle, the bracing, connected to the inner column, buckled in plane of the frame. In contrast with this, the bracing, connected to the outer column, buckled out of plane of the frame at the fourth cycle. After then, local bucklings were observed at both ends and the center of the bracings. Buckling of the bracing caused rapid reduction of the horizontal shear capacity of the frame. The hysteresis loops showed typical mode of braced frame.

Fig.-6 shows the hysteretic relation of the moment and rotation at the exterior end of the composite girder of specimen No.1. In Fig.-6, the moment which gives the compression in concrete slab is taken as positive.

Fig.-7 shows the relation between vertical force P and vertical displacement δv at the center of the span of specimen No.2. The vertical force P is calculated as the difference of the vertical components of the axial forces acting in both bracings. P should be balanced by the shear of girders.

Fig.-8 shows the relation between nodal moment and shear deformation angle of the joint panel of the inner column of spcimen No.1.

In Fig.-9, the relation between axial force and axial displacement of the bracing indicated by bold line is recorded. Axial yielding did not occur in both bracings under tension stress. While, the bracings buckled in turn according to the load reversal, having been accompanied by the subsidence of mid-span of the girder as observed in Fig.-7. Flexural buckling of the bracing caused severe local buckling, and after several times of repetition of local buckling, the bracing had fractured.

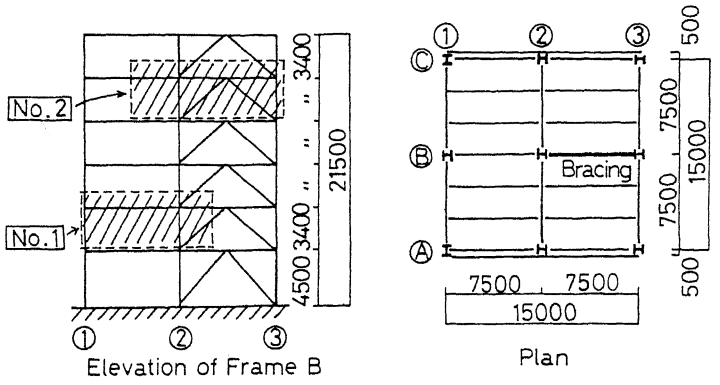

Fig.-1. Plan and Elevation of the Six-Story Steel Building

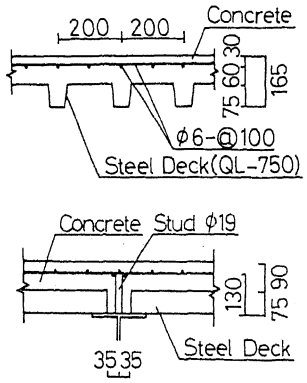

Fig.-2. The Composite Slab

Table-1. Mechanical Property of the Materials

		σ_y	$\sigma_{u,Fc}$	ε_{st}
16WF57	Flange	29.2	43.1	2.17
	Web	38.5	47.7	2.08
14WF30	Flange	29.0	45.5	1.83
	Web	33.7	47.0	2.52
10WF54	Flange	29.8	44.6	2.18
	Web	35.6	49.7	2.09
8WF40	Flange	27.8	43.7	2.42
	Web	30.5	44.4	1.98
Bracing □5"x5"x0.18"		36.4	44.1	1.43
Wire Mesh φ6-100@x100@		36.3	44.7	2.36
Concrete Slab	No.1		2.50	
	No.2		3.10	

σ_y : Yield Stress (kgf/mm²)
σ_u : Tensile Strength of Steel (kgf/mm²)
Fc : Compressive Strength of Concrete (kgf/mm²)
ε_{st}: Strain of Strain-hardening Point (%)

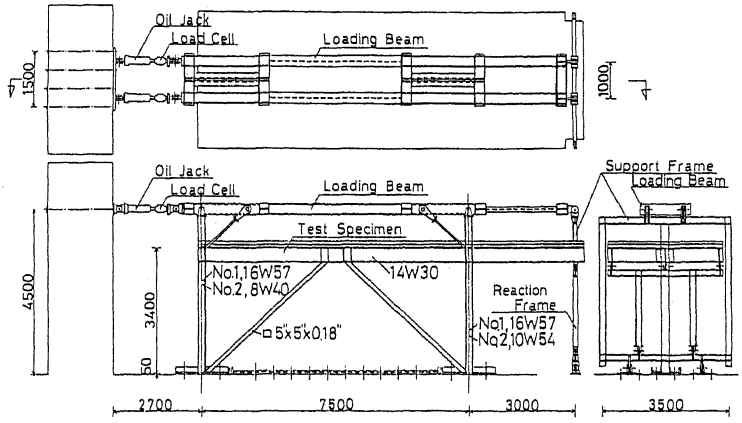

Fig.-3. Loading Scheme

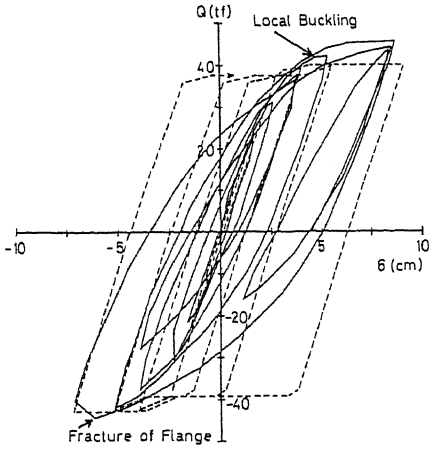

Fig.-4. Q-δ Relation of No.1

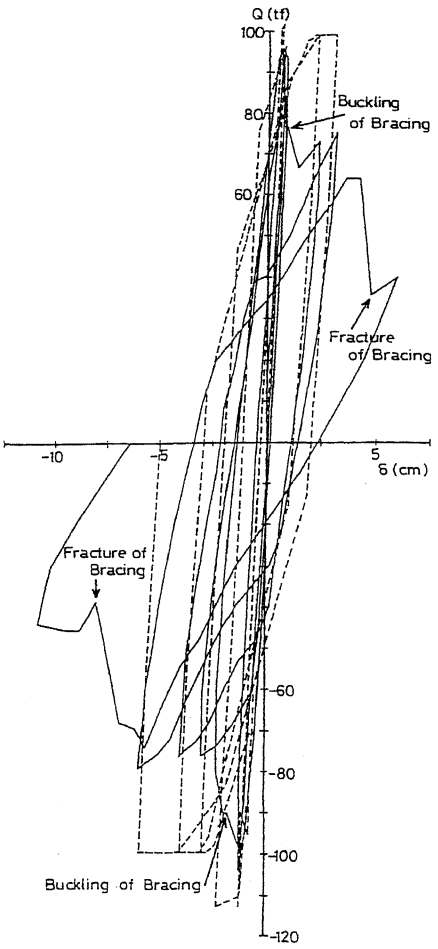

Fig.-5. Q-δ Relation of No.2

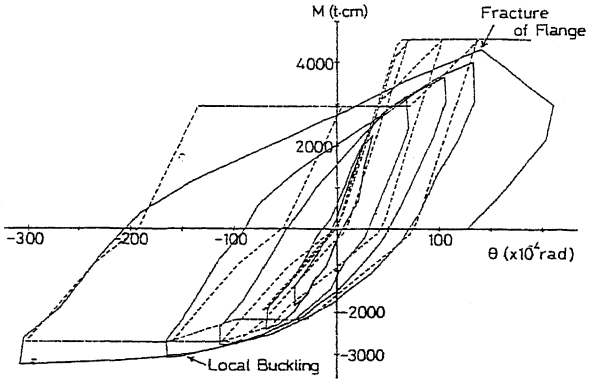

Fig.-6. M-Θ Relation of Composite Girder

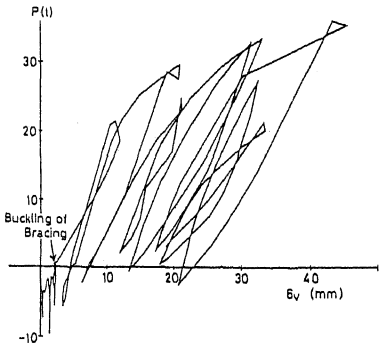

Fig.-7. P-δv Relation of Composite Girder

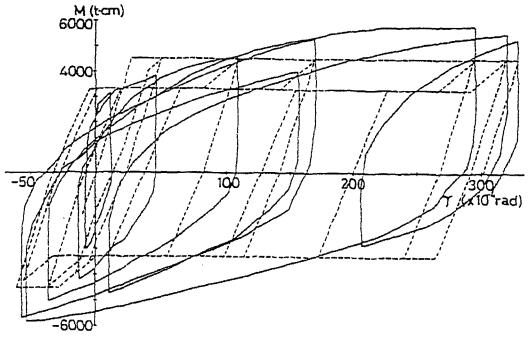

Fig.-8. M-γ Relation of Joint Panel

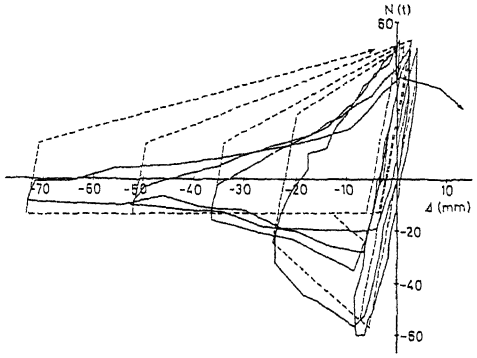

Fig.-9. N-Δ Relation of Bracing

ANALYSIS AND DISCUSSION

Composite Girder

The effective width of concrete slab B, the equivalent moment of inertia Ib and full plastic moment Mbp of a composite girder are given in Eqs.1 through 5 (Ref. 2).

i) Effective width

$$B = b + 2\,be \tag{1}$$

in which $be = \mathrm{Min}[(0.5 - 0.6\,a/l)\,a,\ 0.1\,l]$

b: flange width of steel girder, l: span

a: distance between edges of flanges of adjacent girders (see Fig.10)

ii) Moment of inertia and full-plastic moment for positive bending

$$Ib^{+} = \frac{B\,t}{n}\left[t^2/12 + (Xn^{+} - t/2)^2\right] + Is + As\,(sd - Xn^{+})^2 \tag{2}$$

$$Mbp^{+} = As\,s\sigma y\,(sd - \frac{As\,s\sigma y}{1.7\,Fc\,B}) \tag{3}$$

iii) Moment of inertia and full-plastic moment for negative bending

$$Ib^{-} = Is + As\,(Xn^{-} - sD/2)^2 + Ar\,(sd - Xn^{-})^2 \tag{4}$$

$$Mbp^{-} = Ar\,r\sigma y\,(sd - rd) + b\,tf\,s\sigma y\,(sD - tf) + \frac{tw\,s\sigma y}{4}\left[sD^2 - (\frac{Ar\,r\sigma y}{tw\,s\sigma y})^2\right] \tag{5}$$

in which n: Young's modulus ratio of concrete to steel

Xn^{+}, Xn^{-}: locations of neutral axis for positive and negative bending respectively (see Fig.11)

As, Ar: sectional areas of steel girder and of reinforcing bars

$s\sigma y$, $r\sigma y$: yield points of steel girder and of reinforcing bars

Is: moment of inertia of steel girder

Eqs.2 through 5, the tensile strength of concrete and compressive strength of reinforcing bars are ignored.

The hysteresis rule of composite girder is derived using the following approximate means. The neutral axis of composite girder for positive bending is located approximately at the top surface of steel girder, and the stiffness and full-plastic moment of steel girder and concrete slab respectively are evaluated about this neutral axis. For negative bending,

on the contrary, the neutral axis is located approximately at the centre of web of steel girder, and the stiffness and full-plastic moment of steel girder and reinforcing bars respectively are evaluated about this neutral axis. Hysteresis loops for steel girder and concrete slab thus obtained are shown in Figs.-12(a) and (b) respectively. Finally these two loops are superposed to obtain the hysteresis loops of composite girder as shown in Fig.-12(c).

In Fig.-6, the predicted hysteresis loop of composite girder thus obtained, which is expressed by dashed line, is compared with experimental result.

Joint Panel

Referring to the notations shown in Fig.-13, yield moment of joint panel of a bare steel frame is given as

$$Mpp = \sigma y \, Vp/\sqrt{3} \quad (6)$$

$$Vp = hb \, hc \, tw \quad (7)$$

in which Vp is the effective volume of joint panel.

Effective volume of joint panel of composite girder can be obtained by adding the extra height of (hd + t/2). Namely, the effective height becomes (hb + hd + t/2). However, it should be noted that this composite effect vanishes in the joint panel of outer column when subjected to negative moment. The hysteresis rule for joint panel of composite frame can be constructed by the similar procedure to that described for composite girder as shown in Fig.-14.

In Fig.-8, the predicted hysteresis loop of joint panel in composite girder thus obtained, which is expressed by dashed line, is compared with experimental result. The experimental result is slightly higher than the predicted strength, because the predicted strength is not considered the strain-hardening.

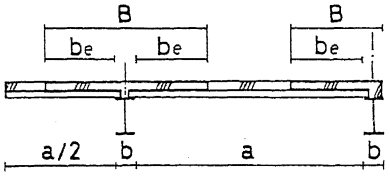

Fig.-10. Effective Width

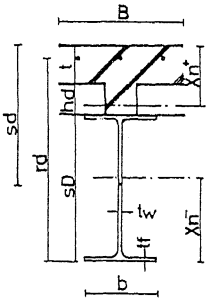

Fig.-11. Section of Composite Girder

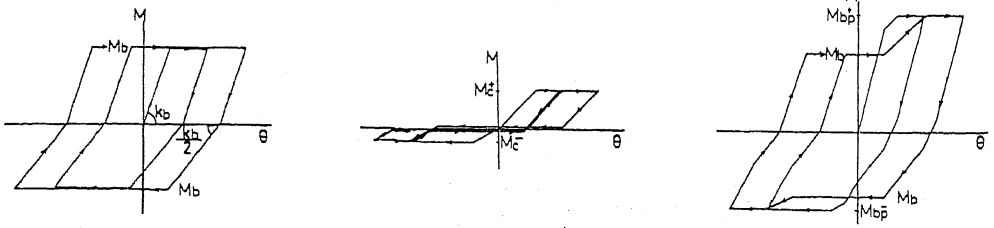

(a) Bare Steel Girder (b) Concrete Slab (c) Composite Girder

Fig.-12. Hysteresis Rule of Composite Girder

Diagonal Bracing

The nominal slenderness ratio of diagonal bracings is 91 assuming both ends are hinged. In reality, considerable restraining effect can be expected at both ends, and roughly estimated effective length factor is 0.65. Namely, effective slenderness ratio could be as low as 59.

The hysteresis rule of diagonal bracing is obtained as following (Ref.3). The axial force vs. axial displacement relationships of a compressive steel bar under monotonic loading can be expressed by three linear segments as illustrated in Fig.-15(a). The characteristic points in this figure are given by the following equations;

$$Ncr = Ny\ [1 - 0.4\ (\frac{\lambda e}{\Lambda})^2]\ /\ [1 + \frac{4}{9}\ (\frac{\lambda e}{\Lambda})^2] \qquad \text{for } \lambda e < \Lambda \qquad (8)$$

$$Ncr = \frac{4}{13}\ (\frac{\pi}{\lambda e})^2\ Ny \qquad \text{for } \lambda e > \Lambda \qquad (9)$$

$$kd = -\ 0.1\ (\lambda e\ \sqrt{\sigma y/E} - 0.75)\ Ab\ E/1' \qquad \text{for } \lambda e\sqrt{\sigma y/E} > 0.75 \qquad (10)$$

$$Nu = Ny/\sqrt{5\ \frac{\sigma y}{E}\ \lambda e^2 + \frac{\pi}{4}} \qquad (11)$$

in which $\Lambda = \sqrt{\pi^2\ E/0.6\ \sigma y}$, λe: effective slenderness ratio, $Ny = Ab\ \sigma y$
Ab: sectional area of bracing, 1': length of bracing

Hysteresis loops of diagonal bracing can be constructed on the basis of monotonic loading curve as illustrated in Fig.-15(b).

In Fig.-9, the predicted hysteresis loop of diagonal bracing thus obtained, which is expressed by dashed line, is compared with experimental result.

Frame

The hysteresis loops of the test frames can be constructed using hysteresis loops of each component. Assuming the inflexion points at mid-span and mid-height of members, the specimen No.1 (moment frame) can be decomposed into four parts as shown in Fig.-16. And hysteresis loop of the moment frame can be constructed by making the horizontal displacement at each nodal points to be compatible.

With respect of specimen No.2, the hysteretic curve of the moment frame and that of diagonal bracings are simply superposed by equating the horizontal displacements. It is assumed joint panel does not yield, because the shear deformation of it is restrained considerably by the force coming from the diagonal bracing.

The predicted hysteresis loops of test frames are seen by dashed lines in Fig.-4 and Fig.-5, respectively. In specimen No.2, the predicted strength at the post buckling stage of bracings is higher than the experimental result. After the buckling of compressive bracings, in the actual frame, the girder was bent down severely, and the tensile bracing did not yield. Such an interaction between moment frame and diagonal bracings are not taken account in this simple analysis, which might caused the discrepancy between the test and prediction.

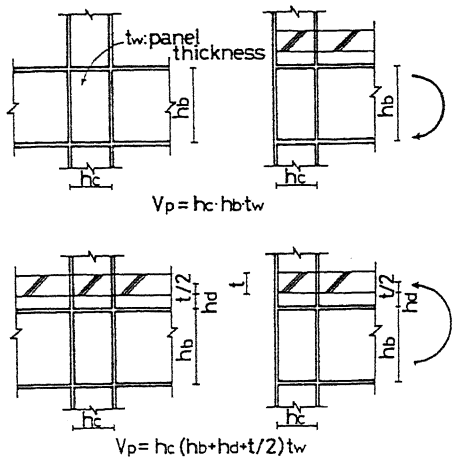

Fig.-13. Analytical Models

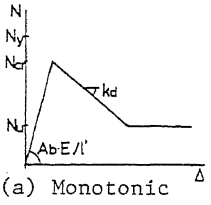

(a) Monotonic

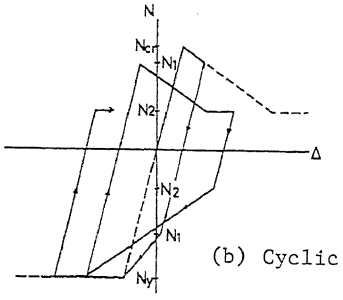

(b) Cyclic

Fig.-15. Hysteresis Rule of Bracing

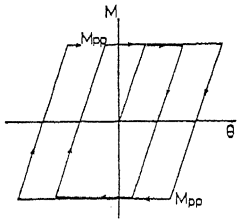

(a) Panel of Bare Steel Frame

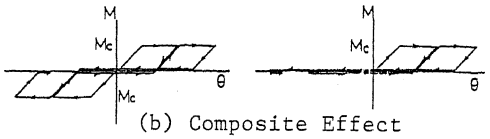

(b) Composite Effect

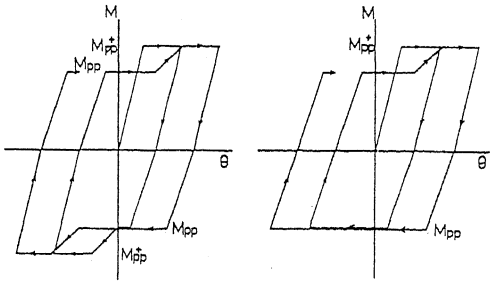

(c) Panel in Inner (c') Panel in Outer

Fig.-14. Hysteresis Rule of Panel

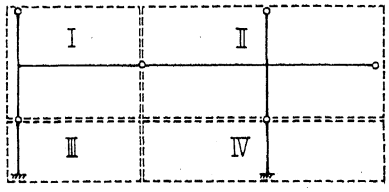

Fig.-16. Decomposed into Four Parts of the Frame

(Ref.1) K.Kamimura, M.Watabe "U.S.-Japan Cooperative Research Program Utilizing Large-Scale Testing Facilities. Full Scale Seismic Tests of a Steel Building and the Supporting Test on it's Half Scaled Partial Frames" 15th Joint Meeting of U.-J. Panel on Wind and Seismic Effect U.J.N.R. Tukuba, May 1983

(Ref.2) Architectural Institute of Japan "Recommendation of Structural Design in Composite Girder" 1975

(Ref.3) B.Kato, H.Akiyama "Restoring-Force Characteristics of Braced Steel Frame" Transaction of the Architectural Institute of Japan No.260 Oct. 1977